This is a pre-print of an article published in **Trees.** The final authenticated version is available online at https://doi.org/10.1007/s00468-018-1660-9.

Title: When the sun never sets: daily changes in pigment composition in three sub-arctic woody plants during the summer solstice

Authors: Beatriz Fernández-Marín[1,*], Albert Porcar-Castell[2], Beñat Olascoaga[2], Jon Atherton[2], Pasi Kolari [3], José I García-Plazaola[1]

***Corresponding author email:** beatriz.fernandezm@ehu.es. **phone:** +34 94 601 5012

Addresses

[1]Department of Plant Biology and Ecology. University of the Basque Country (UPV/EHU). Box 644. E-48080 Bilbao (Spain)

[2]Optics of Photosynthesis Laboratory, Department of Forest Sciences. Latokartanonkaari, 7 PO Box 27, 00014 University of Helsinki, Finland.

[3]Department of Physics, PO Box 68, 00014 University of Helsinki, Finland

Running head: pigment dynamics during sub-arctic summer solstice

Abstract

Composition and content of photosynthetic pigments is finely tuned by plants according to a delicate equilibrium between absorbed radiation and the proportion that photosynthetic apparatus can actually convert into photochemistry. Subarctic and Arctic plants are subjected to extended periods of continuous light during summer what represents a unique natural scenario to study the influence of light and temperature on pigment regulation, and the presence of diurnal patterns potentially governed by circadian rhythms. Here, we examined photosynthetic apparatus modulation of three naturally co-occurring woody species (*Betula pubescens* ssp. *czerepanovii*, *Arctostaphyllos alpinus* and *Pinus sylvestris*) around the summer solstice, at 67º N latitude. Plants received solar radiation continuously during the 3-day experiment although PPFD fluctuated: was lower during subjective-nights. Xanthophyll cycle was active at any time of the day in all the three species but its responsiveness to PPFD was exacerbated during subjective-nights. This was particularly evident for Alpine bearberry that maintained even at subjective-night a highly de-epoxidated state. Its daily oscillations in neoxanthin and α-Carotene were significantly related to the time of the day, what was indicative of circadian regulation. Variations in neoxanthin and carotenes in Scots pine were mainly driven by PPFD and, to lesser extent, by air temperature.

Photochemical efficiency for a certain PPFD was pretty the same during daytime and subjective-nights for the three species. Net assimilation was vaguely higher at daytime than at subjective night in Scots pine, but most of the variance was explained by PPFD (rather than by time of the day).

Overall, dynamism in pigment content was mainly driven by PPFD even at subjective-night. This dynamism was unrelated to day/night cycles: indications of potential circadian regulation were found only in Alpine bearberry. The results could indicate an incomplete acclimation to 24h photoperiod for the studied species that colonize this latitude relatively recently.

Key words: arctic, carotenoid, chlorophyll, circadian rhythm, photochemical efficiency, xanthophyll cycle

Introduction

Through the course of evolution, most living organisms, have adapted to the diurnal fluctuations in solar radiation dose induced by the rotation of the Earth around its axis. Anticipation to predictable environmental conditions is a key mechanism to take advantage of such rhythmic changes. Thus, circadian clocks are present in diverse groups of organisms (from cyanobacteria to vertebrates) (Bell-Pedersen et al. 2005). For example, in the model plant *Arabidopsis* one third of nuclear genes are under circadian control (Covington et al. 2008) regulating most of the physiological processes in plants, including gas exchange and photosynthesis. Under natural conditions, circadian clocks are set every day by environmental events, such as sunrise or sunset.

However, most of these effects are only revealed when plants are transferred to artificially maintained constant environmental conditions, particularly constant light (CL). In this situation, rhythmic physiological patterns appear, although they weaken with time, and are finally lost after several days (McClung 2006, Caldeira et al. 2014, García-Plazaola et al. 2017). CL can cause detrimental damage in plants and some species are not able to survive under a CL regime (Vélez-Ramírez et al. 2011). This is logical since CL *sensu stricto* does not exist on Earth and even around the solstice and at very high latitudes, when photoperiod is 24-h, there are considerable diurnal variations in light intensity and spectral quality. Nevertheless, Arctic and Antarctic environments above 60º latitude differ from the rest of terrestrial ecosystems by the fact that they are exposed during a variable period of time along the year (summer) to continuous light, when sun never sets.

Despite the importance of arctic and sub-arctic ecosystems on Earth, where they occupy vast extensions, and despite their susceptibility under a climate change scenario, plant photosynthetic responses in these environments are surprisingly poorly characterised. A recent study shows that diurnal cycles of photosynthesis in arctic plants are under circadian control (Patankar et al. 2013), but it has not been clearly established whether arctic plant communities are able to take advantage, in terms of carbon gain, of this 24-h photoperiod in summer. Interestingly, a recent study on the responses to CL in tomato cultivars (Vélez-Ramírez et al. 2014) showed that the northernmost varieties of tomato were less susceptible to CL (e.g. higher photochemical efficiency and less leaf chlorosis). These authors showed that the higher tolerance of these cultivars to CL was related with a single gene encoding a light harvesting chlorophyll a/b-binding protein

(Vélez-Ramírez et al. 2014). In agreement with such observations, annual plants transferred from an oscillating environment to CL show a robust 24-h rhythm on chlorophyll content (Pan et al. 2015, García-Plazaola et al. 2017), so it is possible that the adjustments on antenna size and composition and balance in the light harvesting by PSI and PSII are essential in the adaptation to long photoperiods. Due to higher difficulties for manipulation under controlled conditions, much less information is available with regard to woody species. Nevertheless, the scarce literature available about changes in photosynthetic pigment content after transference of plants to CL, indicate rhythmic oscillations in chlorophyll content in woody species too, such as *Gossypium hirsutum* (García-Plazaola et al. 2017).

One of the most remarkable features of plant pigments is that their composition and proportion is highly dynamic, reflecting changes in photosynthetic processes. In particular, on a daily scale, cycles of synthesis/degradation of components of the light harvesting complexes (chlorophylls) (Fukushima et al. 2009; Garcia-Plazaola et al. 2017) and inter-conversion of xanthophylls within the violaxanthin (V) cycle (Demmig-Adams and Adams 1996) occur. The latter consists on the light-induced conversion of V into zeaxanthin (Z). In darkness, or during the night, the opposite reaction takes place, giving rise to the so-called V-cycle that usually operates following a daily rhythm. This cycle modulates the efficiency of light energy conversion by the photosynthetic apparatus, preventing its damage under conditions of light energy absorbed in excess. As a result, because the kinetics of conversion between V and Z operate at time scales of minutes, the V-cycle can have a significant effect on plant productivity under fluctuating light (i.e. presence of clouds), with up to 20% reduction in photosynthetic carbon uptake (Kromdijk et al. 2016).

Pigment composition and dynamics have been rarely studied in arctic plants where circadian controls might be partly offset due to high latitude dynamics in solar elevation. As an example, in a recent meta-analysis compiling data from more than 500 studies about plant pigment composition and dynamics (Esteban et al. 2015), none of them was performed at latitudes higher than 67°N and only 3 studies at latitudes above 60º. In the present study we aim to characterise the daily changes in pigment composition in three subarctic woody plant species (comprising trees and shrubs) and their impact on daily patterns of photosynthetic capacity under a natural 24-h photoperiod, above 67°N. We study as representative of the main life forms a conifer, Scots pine (*Pinus sylvestris* L.); a deciduous broadleaf tree, mountain birch (*Betula pubescens* ssp. *czerepanovii* (N.I.Orlova) Hämet-Ahti); and a dwarf cushion shrub, alpine bearberry (*Arctostaphyllos alpinus* (L.) Nied.). We hypothesize that: (i) photosynthetic pigments show daily changes comparable to those of lower latitude plants mainly driven by PPFD, (ii) the xanthophyll cycle is active during a "subjective night" (i.e. the 6 h period around midnight from 9 pm to 3 am Eastern European Time: EET), and (iii) pigment composition and photosynthetic capacity relate differently under day vs. subjective nights periods.

Methods

Plants and study site

Field measurements were performed at Värriö Strict Nature Reserve (Lapland, Finland) (67°44'N. 29°36'E) in June 2016. The area lies in the boreal zone in north-eastern Finland and it is mostly covered by a natural subarctic pine forest. Annual average temperature in the nearby Station for Measuring Ecosystem-Atmosphere Relations (SMEAR-I) at "Värriö Strict Nature Reserve" is -0.5 °C, and during the week of summer solstice the average maximum and minimum temperatures of the last 10 years are 17 °C and 7 °C, respectively.

The study site was a gentle slope facing north (elevation of 460 m), just above the arctic timberline, so it potentially can receive direct sunlight during 24h in the summer solstice, being the exposition to sunlight favoured at night by its northern orientation. Two consecutive daily cycles (from 13:00 June 21st to 10:00 June 23rd) were followed around the solstice, with eleven time points distributed along this period (Fig. 1). Thus, two subjective night periods (from the 21st to the 22nd, and from the 22nd to the 23rd of June) were considered during the study. As previously pointed out, there is no real night at this period of the year at this latitude and the time comprised between 9 pm and 3 am was considered as "subjective night". The first subjective night during the experiment was mainly cloudy with a low PPFD and the second one was predominantly sunny (Fig. 1).

Three woody species were studied: Scots pine (*Pinus sylvestris*), a conifer just in its ecological limit; mountain birch (*Betula pubescens* ssp. *czerepanovii*), a broadleaf deciduous tree; and alpine bearberry (*Arctostaphyllos alpinus*), a dwarf cushion shrub with broadleaves and deciduous habit. Four individuals of each species were selected for the experiments. Scot pines were approximately 4 m tall and only needles from 2014 cohort were sampled. Mountain birches were about 1.5 m tall, and alpine bearberry grew up to 5 cm above the ground. Leaves were always collected from North expositions with slight differences on light environment caused mainly by the differential crown architecture of each species. Thus, the percentage of canopy transmittance (also called canopy openness) for the studied leaves was 98.0±0.9 (average ± SE of four individuals) for bearberry, 86.8±3.6 for mountain birch and 75.2±3.5 for Scots pine. This parameter was calculated through the software Canopy Gap Analyser (CGA) version 2.0. Hemispherical images were taken with a digital camera Nikon Coolpix 4500, equipped with a fisheye lens FC-E8. Images were processed with CGA to transform image pixel intensities into sky and non-sky areas. Based on geographical coordinates of the location, the software further calculates the pathway of the sun in the sky dome and finally estimates the year average gap light transmission index in percentage, were 100% would correspond to an object fully exposed to direct sun radiation.

Sampling for pigments and HPLC measurements

Around 25-60 mg (dry weight) of foliar material were taken with a cork borer (for broadleaf species) or cut with scissors (for pine needles), from 2 to 4 different leaves from each individual (4 plants per species) and immediately frozen in liquid nitrogen. In the lab, samples were freeze-dried and stored with silica until biochemical analysis.

For pigment analysis two consecutive extractions were done, the first one with acetone (95%) and the second one with pure acetone (all acetone solutions buffered with 0.5 g $CaCO_3$ L^{-1}). Plant material was ground under liquid N_2 and the extracts were centrifuged at 16100 g and 4 °C. The pellet was then re-suspended in pure acetone, mixed in a vortex and centrifuged again. Both supernatants were pooled together and pigment composition was analysed by HPLC as described previously (García-Plazaola et al. 1999) using a photodiode array detector.

Chlorophyll a fluorescence measurements

Chlorophyll *a* (Chl*a*) fluorescence was measured in the field using a portable modulated PAM-2500 fluorometer (Walz, Effeltrich, Germany), in four plants per species and timepoint. In dark-adapted leaves (30 min) the maximal Chl*a* fluorescence (F_m) was induced with a saturating pulse (0.8 s duration, 8000 μmol m^{-2} s^{-1} intensity) while the initial fluorescence (F_o) was recorded with low measuring light intensities (ML<1 μmol photons m^{-2} s^{-1}, ML-frequency=200 Hz). The F_v/F_m was then estimated by the ratio $F_v/F_m = (F_m - F_o)/ F_m$.

The operating quantum efficiency of PSII (ΦPSII) was measured by using the light clip of the PAM-2500 (Leaf-Clip Holder 2030-B, Walz GmbH, Effeltrich, Germany) In illuminated leaves (i.e. directly exposed to natural solar radiation) the operating quantum efficiency of PSII was estimated as $\Phi PSII=(F_m'- F_s)/ F_m'$, where F_m' is the maximal Chl*a* fluorescence induced with a saturating pulse (0.8 s) and F_s is the actual Chl*a* fluorescence under illumination. During ΦPSII measurements, natural PPFD was recorded measured with the PAR sensor of the Leaf-Clip (Micro-Quantum-Sensor, Walz GmbH, Effeltrich, Germany) that was then used for ETR estimation. Actual PPFD ranged between 14 and 1541 μmol photons m^{-2} s^{-1} during the experiment.

Meteorological data and CO_2 exchange

Data about air temperature, PPFD of the site of study, and on CO_2 flux from Scots pine were obtained from the SMEAR-I research station (Station for Measuring Ecosystem Atmosphere Relations). The station is located on a hilltop at the timberline (elevation 400 m). Air temperature and PPFD were measured in a tower at 2 m height and at 1-min intervals with Pt100 sensors and Li-190 PAR sensor (Li-Cor Inc., Lincoln, Nebraska, USA), respectively.

SMEAR I is surrounded by relatively homogeneous Scots pine stand with density of about 700 trees/ha. The studied trees were 60–70 years old and 8–10 m tall. CO_2 exchange of pine shoots was measured with four chambers that were installed near the top of tree crowns. Each chamber accommodated one shoot with one or two age classes of needles in the branch tip. The shoots were gently bent into horizontal plane to improve the correspondence of light conditions experienced by the shoot with the measurement on incoming PPFD. The chambers were open most of the time for the enclosed shoots to experience near-ambient conditions. Each chamber was closed for one minute every 10 min, CO_2 fluxes were calculated dynamically from the change in CO_2 concentration inside the closed chamber. The details of the chamber measurements can be found in Kolari et al. (2007). The fluxes are given for all-sided needle area. All meteorological and chamber data are available in SMEAR database at http://avaa.tdata.fi/web/smart/smear.

SMEAR-I station was located approximately 1km away from the sampling plot. Air temperature and PPFD data from SMEAR-I was averaged for a period of 90 minutes around each sampling timepoint for pigment and Chl fluorescence analysis. Sampling took approximately 60 minutes and we incorporated an extra 30 minutes prior to sampling to get a more representative number for PPFD and temperature. We assumed that this averaging cancelled out any potential variation in PPFD and temperature between sampling plot and the nearby SMEAR-I station. These averaged PPFD and temperature values were later on used to construct the statistical models and assess the role of temperature, radiation and solar zenith angle on pigment modulation.

Additionally, diurnal average PPFD was estimated for the summer solstice week (time interval between 18^{th} of June at 00.00h and the 24^{th} of June at 00.00) compiling the data of the last 15 years: from 2001 to 2016. CO_2 fluxes in Scots pine were also compiled for the same time interval from SMEAR-I. Only values measured at temperatures in the range 10-15 °C were considered. Day and subjective night data were separately analysed. Subjective night was considered as a 6 h interval comprised between three hours before (9 pm) and three hours after midnight (3 am).

Statistical analyses

One-way ANOVA followed by Duncan's post hoc test was used to test for differences in the content of photosynthetic pigments (i) among the three analysed species, (ii) among different timepoints during measurements and (iii) before and after a nocturnal sunbeam, after checking homoscedasticity of data. Some parameters showed heteroscedasticity even after data transformation. In these cases, the non-parametric Kruskal-Wallis H-test was applied, followed by multiple pairwise comparisons with Mann-Whitney U-test. Pearson's correlation was applied to analyse the relationship between AZ/VAZ and F_v/F_m. When correlation was significant, a linear regression model was applied. These statistical analyses were conducted using the SPSS 24.0 statistical package at a significance level of $\alpha = 0.05$.

In addition, we examined the linear relationships between environmental, biochemical and photochemical factors by calculating Pearson correlation coefficients between variables. To expand this, and in an attempt to examine the impact of circadian cycles on the leaf pigment concentration dynamics in the presence of fluctuating environmental conditions, we analysed the pigment data using three linear models and a hierarchical (ordered) approach. The first model used only the average PPFD described above (M1). The second model used both average PPFD and Temperature (M2). In addition to PPFD and Temperature, the third model included also circadian control using solar zenith angle as a proxy (M3). The solar zenith angle for each measuring time was calculated using the R using 'solarPos' package, and then normalised between 0 (maximum angle at solar midnight) and 1 (minimum angle at solar noon). We assessed the significance of each model by comparison with the previous (simpler) model in the hierarchy, using an F-test and a false rejection level (α) of 0.05. For example, M2 was compared to M1, and M1 was compared to the null model (no relationship). To assess the significance of estimated parameter values, we applied t-tests. Again, α was set to 0.05. We also visually examined model predictions and residuals for those models whose F-test results were within the false rejection threshold, i.e. those that were deemed statistically significant, to check for undue influence of outliers. This section of the analysis was conducted in the R language.

Results

Weather conditions

During the week previous to the study the weather was in general cloudy with average maximum temperature of 16.5°C and minimum of 7.5 °C (Fig. 1). In the two consecutive daily cycles of the study period temperatures oscillated between 18.0 °C and 7.8 °C. Irradiance was always higher than zero, minimum recorded value was 2 $\mu mol\ m^{-2}\ s^{-1}$ PPFD, reaching 1750 $\mu mol\ m^{-2}\ s^{-1}$ PPFD during periods of direct sunlight at noon. The first subjective night was cloudy and midnight irradiance was 6-7 $\mu mol\ m^{-2}\ s^{-1}$ PPFD, while the second subjective night was sunny and PPFD was never lower than 20-22 $\mu mol\ m^{-2}\ s^{-1}$ (Fig. 1 inset).

Daily changes in pigment composition

Characterisation of photosynthetic pigment composition for the three studied species is shown as average of the 11 sampling timepoints in Figure 2. Chlorophyll (Chl) content was half (expressed on dry weight basis) and Chl a/b ratio was slightly lower in pine needles than in the two angiosperms species (Fig 2a). As these differences probably reflect architectural differences among the studied species, to allow easy comparison, all carotenoids were expressed in relation to chlorophyll content. For Scots pine, relative concentrations of neoxanthin (Neo/Chl), lutein (Lut/Chl) and β-carotene (β-Car/Chl) were significantly higher than in the other two species (Fig 2b), while the ratio of total pool of xanthophyll cycle pigments to Chl (VAZ/Chl) was comparable for the three species. Alpine bearberry differed from the other angiosperm, mountain birch, in slightly but significantly higher β-Car/Chl, Chl a+b and Chl a/b and by slightly lower Lut/Chl contents.

Pigment contents varied along the course of the study period at different extent in the three species (Fig. 3). In pine needles all carotenoids peaked during the first hours of the daily cycle (1 to 7 am). In mountain birch there was a trend towards a negative adjustment of carotenoid pools during the course of measurements, while in alpine bearberry pigment ratios were fairly stable (Fig. 3 a-c). Absolute Chl content showed the largest oscillations (from a minimum of 3.6 to a maximum of 4.2 $\mu mol\ g^{-1}DW$) in mountain birch (Fig 3d). Thus, Chl a+b was maximum (3.61 to 4.2) around each noon (Fig 3d: around 25 and 45h after experiment started). Chl a+b variations were much buffered in the other two species, oscillating between 2.8 and 3.2 in alpine bearberry and between 0.9 and 1.5 in Scots pine. For Scots pine, only the first point was clearly higher (1.5 ± 0.11), being the rest of timepoints below 1.3 μmol g^{-1} DW.

In contrast to the modest oscillation of the rest of carotenoid ratios, both the pool of VAZ pigments, as well as its de-epoxidation state (AZ/VAZ) were highly dynamic (Fig 3 e, f), particularly in the two angiosperms. Thus, AZ/VAZ was the only parameter showing statistically significant differences among timepoints in all the three species (Supplementary Table S1). The ratio VAZ/Chl oscillated between 31 and 89 mmol mol^{-1} Chl in alpine bearberry and between 39 and 81 in mountain birch, while in Scots pine VAZ/Chl ranged between 43 and 61 mmol mol^{-1} Chl (Fig. 3e). Despite this strong variation, VAZ/Chl did not follow a clear pattern of daily oscillation, except for alpine bearberry where VAZ pool tended to decrease during subjective nights and to peak at noon (Fig. 3e). In contrast, AZ/VAZ peaked during the day in the two angiosperms, while in Scots pine there was a trend towards an increase with progression of the study but without daily oscillations (Fig. 3f). In the case of alpine bearberry VAZ/Chl and AZ/VAZ were significantly and positively correlated (Pearson's correlation coefficient 0.87, $P<0.001$, data not shown). For this species was particularly remarkable the high level of de-epoxidation maintained throughout the experiment, that was never lower than 0.54 (Fig. 3f).

For a deeper assessment of the influence of the air temperature, the PPFD and the time of the day on photosynthetic pigment contents and photochemistry a hierarchical linear regression analysis was performed (Table 1 and Fig. 4, see also supplementary tables S3, S4 and S5). When the effect of each individual variable was evaluated separately, and as evidenced by the highest correlation coefficients, Scots pine appeared, in principle, as the species with a strongest potential circadian rhythm (Fig. 4). This was particularly remarkable for α- and β-Car that correlated negatively with the "solar angle" (e.g. decreased towards midday, higher irradiances, and higher temperature) and also for Chl a+b and Chl a/b that correlated positively (e.g. tended to increase at midday) (Fig. 4c).

However, since "solar angle" was strongly correlated with PPFD and to some extent also with temperature (Fig. 4) it was not possible to separate effects with the correlation analysis alone. To this end we constructed three different models based on PPDF (M1), PPFD + Temperature (M2) and PPFD + Temperature + Normalised solar zenith angle (M3). We expected that for pigments that have a strong circadian cycle adding the variable "solar angle" would result in a significant improvement of the model. Alpine bearberry was the only species where the effect of circadian rhythms could be observed for Neo/chl and α-Car/Chl (Table 1). Conversely, photosynthetic pigment fluctuations in mountain birch and Scots pine, appeared as mainly regulated by PPFD and air temperature (Fig. 4a, c, Table 1).

Effect of a "sunbeam" at night

The night period from June 22 to June 23 was initially cloudy but between 20:30 and 22:00 cloudiness disappeared and sunlight illuminated directly the leaves. This occurred two hours before midnight so irradiance was not at the lowest value, increasing from 80 to 150 µmol m^{-2} s^{-1} PPFD at the meteorological station (Fig 5a) and even higher in sun-oriented leaves reaching more than 150 µmol m^{-2} s^{-1} PPFD. When this phenomenon occurred air temperature was relatively warm (12-13 °C), allowing the observation of rapid metabolic responses. We took advantage of such unexpected situation and analysed pigment contents immediately before and during direct sunlight illumination (Fig. 5b-g). After 30 minutes of illumination AZ/VAZ increased in the three species, particularly in mountain birch (from 0.43 to 0.66) (Fig. 5g). Furthermore, there was a general activation of carotenoid biosynthesis (particularly of Lut and VAZ; Fig. 5e, f), which resulted on an overall increase in total carotenoids of 10.8%. 4.3% and 6.7% in alpine bearberry, mountain birch and Scots pine, respectively (Fig. 5b). No significant change was observed for any of the three species in the content of Neo or β-Car as a result of the nocturnal sunbeam (Fig. 5c, d).

Daily changes on photochemical efficiency

In parallel to pigment sampling Fv/Fm was measured in dark-adapted leaves and ΦPSII on illuminated leaves (data not shown). There were differences among species in the magnitude of Fv/Fm (0.80-0.83 in pine, 0.72-0.76 in bearberry and 0.71-0.77 in birch), but in each of them the highest Fv/Fm was measured during the first night when the lowest irradiance occurred. In birch Fv/Fm and AZ/VAZ correlated linearly and negatively both during the day and during the subjective night (Fig 6). The correlation between Fv/Fm and AZ/VAZ was weaker, and only evident during daytime in bearberry, while no significant correlation was found for Scots pine. Similarly, AZ/VAZ strongly correlated with ΦPSII in birch, while this correlation was weaker in bearberry and did not exist on pine (data not shown).

We further compared the response of ETR to PPFD between the periods of day and subjective nights. In Fig. 7 the initial (linear) part of the response curve of ETR to PPFD is shown. The slope of the relationship differed among species, being higher in Scots pine. When daytime hours and the hours comprising the subjective night were compared, slightly difference between both slopes was found to be significant only for mountain birch (supplementary Table S2).

Gas exchange

Taking advantage of the data available in the SMEAR-I, we further assessed the response to natural continuous light conditions of one of the species: the Scots pine. Its changes in CO_2 flux in relation to natural irradiance around solstice of the last 15 years (2001 to 2006) are shown in Fig. 8. To avoid an interaction with temperature and help for a better interpretation of the results, only data corresponding to ambient temperature between 10-15 ºC were evaluated. Panels *a* and *b* from Fig. 8 show that maximal PPFD and CO_2 flux peak at noon in Scots pine for a typical day around the solstice. Maximal CO_2 flux is about 200-250, and the probability of negative fluxes is very low between 06.00am and 06.00pm (Fig. 8a). When the initial slope (linear part) of the CO_2 flux vs. PPFD curve are analysed separately for subjective night (e.g. datapoints obtained between 09.00 pm and 03.00 am) vs. day, only slightly differences were observe in the slope that was a bit steeper at day 0.0090 vs. 0.0079 at subjective night. Nevertheless, the factor “day/night” explained only 4% of the variance vs. 28% explained by PPFD (see ANCOVA results in supplementary Table S3). This means slightly higher CO_2 fluxes for the same irradiance occur at day than at subjective nights for Scots pine.

Discussion

Photosynthetic pigment composition and dynamics in arctic and sub-arctic plants has rarely been studied. To the best of our knowledge only one recent publication describes in detail carotenoid composition in leaves of *Salix pulchra* in northern Alaska tundra (68°63'N) (Boelman et al. 2016) and, at a much higher latitude (Spitsbergen 78°04'N) bulk carotenoids and chlorophylls have been studied in a couple of bryophytes, lichens and vascular plants, but by non-resolutive spectrophotometric techniques (Shmakova 2010). In the three species analysed in our work, pigment composition (Fig. 2) fitted within the 95% confidence interval of non-stressed plants recently compiled by Esteban et al. (2015), being the contents of Lut and β-Car in pine needles in the upper part of that interval. Furthermore, pigment stoichiometry, that is determined by the structure of the light harvesting apparatus (Kouril et al. 2013), was remarkably similar among the three species, in particular between the two angiosperms (Fig. 2), indicating, as confirmed by light regime analysis with hemispherical photography, that light environment was similar for the studied branches of the three species. All these observations suggest that, in summer, pigment composition in leaves of sub-arctic plants is not different from that of other angiosperms and also that the studied species were not particularly stressed during this period.

Nonetheless, pigment composition was far from being stable along time and a continuous rearrangement of carotenoid stoichiometry was observed (mainly in VAZ xanthophylls), particularly in needles of Scots pine, but also for the other species (Fig. 3). In general, ratios of individual carotenoids to Chl peaked during the first measurements of the day around the early morning hours upon an increase in solar radiation and when temperatures were comparatively low in relation to daytime (Fig. 1). This was particularly noticeable in pine needles for the case of Neo and Lut, which oscillated with a period close to 24 h. Since Neo content is tightly controlled by the availability of binding sites in outer trimeric light harvesting complexes (LHCII) (Morosinotto and Bassi 2012), this would indicate a down regulation of antenna size (mediated by degradation of trimeric LHCII) during the morning. Whether these oscillations are controlled by internal rhythms or simply respond to environmental fluctuations, it could not be conclusively answered within the limitations placed by our reduced number of observations. Longer future field experimental campaigns where data is acquired at a broader range of times, temperatures and radiation levels might help in tearing apart the contributions of instantaneous PPFD and temperature from those of circadian rhythms for different pigments. However, the fact that the model including the circadian variable (Table 1, M3) significantly increased the percentage of explained variability in Neo/Chl and α-Car/Chl in Alpine bearberry, suggests that circadian rhythms might indeed contribute to the observed diurnal dynamics and play a significant ecophysiological role under natural conditions. Conversely, the most dramatic variation was observed for the case of VAZ to Chl ratio, particularly in alpine bearberry, with an amplitude close to 3 fold between minimum and maximum values. In this sense, is remarkable that VAZ pigments, in particular Z, differ from the rest of xanthophylls by the fact of being not necessarily bound to proteins (Dall'Osto et al. 2007; Havaux et al. 2007), playing additional roles on membrane stabilization (Havaux and García-Plazaola 2014). This may explain why Scots pine and Alpine birch were able to keep relatively high photochemical efficiency despite AZ/VAZ was never relaxed during the experiment (i.e. minimum de-epoxidation index was above 0.4 for both species). Similar dissociation between accumulation of de-epoxidised xanthophylls and Fv/Fm values has also been found for overwintering evergreens (Míguez et al. 2017) what, in sum, reinforces a potential role of zeaxanthin beyond energy dissipation. VAZ/Chl content responded positively to PPFD in the three species and this correlation was stronger than those to temperature or time of the day (Fig. 4) indicating a major control of light intensity over the size of the total VAZ pool.

Pool size and, to higher extent, de-epoxidation state of the xanthophyll cycle (VAZ/Chl and AZ/VAZ, respectively), were strongly and negatively correlated with ΦPSII and F_v/F_m in alpine bearberry and mountain birch (Fig. 4a, b, 6a, b). Conversely, no significant correlation was found with F_v/F_m for Scots pine (Fig. 4c and 6c) what could indicate a faster mechanism for re-epoxidation of xanthophylls in this species. Scots pine showed, in addition the highest levels of F_v/F_m during the experiment (Fig. 6), despite having VAZ content similar to that of the other two species (Fig. 2). Higher assimilation capacity in pine vs birch species have been related to higher Fv/Fm, thermal dissipation and antioxidants levels as part of improved photoprotection mechanisms in conifers cohabiting with birch in alpine environments (Fernández-Martínez and Fleck, 2016). The differences we found for Fv/Fm in Scots pine, in comparison with the other two species might indicate the operation of different photoprotection mechanisms for perennial needles vs deciduous leaves but could also reflect the intrinsic variation in summer F_v/F_m levels previously observed across species

(Björkman & Demmig 1987), including Scots pine and Silver birch (Atherton et al. 2017).

Recent studies have shown the existence of a robust circadian rhythm of photochemical efficiency in wild barley, Arabidopsis, bean and cotton (Dakhiya et al. 2017, García-Plazaola et al. 2017, Litthauer et al. 2015). These findings open the simple question of whether arctic plants "sleep" during the midnight sun period or maintain the same environmental regulation of photosynthetic activity as during daytime. At this regard, Patankar et al. (2013) showed that photosynthesis and respiration in several tundra plants were controlled by some degree of circadian regulation. To test whether such control is also exerted over photochemical processes, the slope of the initial (linear) part of the PPFD vs. ETR relationship was compared at daytime and at a subjective night period (Fig. 7). Clearly, no differences were observed between both adjustments, which suggests that the impact of circadian rhythms in foliar pigment contents and photosystem structure would not play a significant role in leaf photochemistry. This was further supported when the initial (linear) part of the PPFD vs. CO_2 flux curve were compared between day and subjective night periods, since no big difference was observed in the slope (Fig. 8c, d). In sum, arctic/sub-arctic plants might be able to capitalise from increasing air temperature also during night because the circadian control of photochemistry is apparently not significant.

Under non-stressful conditions, particularly when night temperatures are above zero, an almost complete re-epoxidation of VAZ cycle pigments occurs in most, if not all, plant species studied under field conditions (Míguez et al. 2015). Thus, predawn values of AZ/VAZ are typically lower than 0.3 in non-stressed plants. Though, this was not the case of the present study, where AZ/VAZ was almost constantly higher than 0.5 in leaves of alpine bearberry and Scots pine despite relatively high values of F_v/F_m were measured concomitantly (≥0.72 and ≥0.80, respectively). Even during the subjective night periods (particularly the second subjective night), AZ/VAZ did not relaxed in these two species (Fig. 3), being close to 1 in bearberry during the second, sunny subjective night. Furthermore, the change in light intensity, caused by cloud opening during the second subjective night, exacerbated even more the VAZ cycle activity in the three species (Fig. 5). This indicates that, despite the circadian regulation in the expression of the enzymes involved in VAZ interconversions (VDE and ZE) (Zhao et al. 2012; Covington et al. 2008; Audran et al. 1998), the cycle operates during night-time with apparently the same efficiency, as a direct response to increasing absorbed light intensity. Furthermore, given that the variation on PPFD observed during the mentioned sunbeam, which accounted for an increase of 70 µmol m^{-2} s^{-1} (Fig. 5), is 20-fold lower than midday PPFD (1800 µmol m^{-2} s^{-1}, Fig. 1), it seems that the xanthophyll cycle operation is more sensitive to irradiance during night-time. Whether this is a specific adaptation of high-latitude ecotypes, a general trait in plants, or the consequence of damage caused by continuous illumination during night, or a reflection of the different temperature regime between day and night, remains to be clarified.

Continuous light can be detrimental for plants, but arctic ecosystems are naturally exposed to a 24 h photoperiod for weeks or even months. Oscillations in light intensity and quality in the arctic summer are probably high enough to set the circadian clock (Velez-Ramirez et al. 2011), but the absence of complete darkness triggers an incomplete relaxation of xanthophyll cycle, dramatic in the case of bearberry, indicating that some arctic plants spend all the 24 h photoperiod in a highly dissipative state, thereby with reduced assimilation rates. This could be interpreted as a lack of complete adaptation to long photoperiods due to their recent arrival at very high latitudes (after the last glacial period), so evolution has been unable to develop physiological solutions to this particular situation, after last ice age (Pedersen 1990). Alternatively, sustained AZ/VAZ could represent a successful conservative strategy to anticipate events of low temperatures potentially frequent at these latitudes even during the summer time.

Acknowledgments

Non applicable

Funding

Basque Government (UPV/EHU IT-1018-16); Spanish Ministry of Economy and Competitiveness (MINECO) and the ERDF (FEDER) (CTM2014-53902-C2-2-P and Juan de la Cierva-Incorporation fellowship IJCI-2014-22489 to B.F-M.); Finnish Academy (272041 and 293443); Funds of the University of Helsinki (490116).

References

Atherton J, Olascoaga B, Alonso L, Porcar-Castell A (2017) Spatial variation of leaf optical properties in a boreal forest is influenced by species and light environment. Front Plant Sci. doi: 10.3389/fpls.2017.00309

Audran C, Borel C, Frey A, Sotta B, Meyer C, Simonneau T, Marion-Poll A (1998) Expression studies of the zeaxanthin epoxidase gene in *Nicotiana plumbaginifolia*. Plant Physiol 118:1021-1028.

Bell-Pedersen D, Cassone VM, Earnest DJ, Golden SS, Hardin PE, Thomas TL, Zoran MJ (2005) Circadian rhythms from multiple oscillators: lessons from diverse organisms. Nat Rev Genet 6:544-556.

Björkman O, Demmig B (1987) Photon yield of O2 evolution and chlorophyll fluorescence characteristics at 77 K among vascular plants of diverse origins. Planta 170:489-504

Boelman NT, Magney TS, Logan BA, Griffin KL, Eitel JUH, Greaves H, Prager CM, Vierling LA (2016) Spectral determination of concentrations of functionally diverse pigments in increasingly complex arctic tundra canopies. Oecologia 182:85-97.

Covington MF, Maloof JN, Straume M, Kay SA, Harmer SL (2008) Global transcriptome analysis reveals circadian regulation of key pathways in plant growth and development. Genome Biol 9:R130.

Dakhiya Y, Hussien D, Fridman E, Kiflawi M, Green R (2017) Correlations between circadian rhythms and growth in challenging environments. Plant Physiol 173:1724-1734.

Dall’Osto L, Cazzaniga S, North H, Marion-Poll A, Bassi R (2007) The Arabidopsis aba4-1 mutant reveals a specific function for neoxanthin in protection against photooxidative stress. Plant Cell 19:1048-1064.

Demmig-Adams B, Adams WW (1996) The role of xanthophyll cycle carotenoids in the protection of photosynthesis. Trends Biochem Sci 1:21-26.

Esteban R, Barrutia O, Artetxe U, Fernández-Marín B, Hernández A, García-Plazaola JI (2015) Internal and external factors affecting photosynthetic pigment composition in plants: a meta-analytic approach. New Phytol 206:268-280.

Fernàndez-Martínez J, Fleck I (2016) Photosynthetic limitation of several representative subalpine species in the Catalan Pyrenees in summer. Plant Biol 18:638-648.

Fukushima A, Kusano M, Nakamichi N, Kobayasho M, Hayashi N, Sakakibara H, Mizuno T, Saito K (2009) Impact of clock-associated Arabidopsis pseudo-response regulators in metabolic coordination. P Natl Acad Sci USA 106:7251-7256.

García-Plazaola JI, Becerril JM (1999) A rapid HPLC method to measure lipophilic antioxidants in stressed plants: simultaneous determination of carotenoids and tocopherols. Phytochem Analysis 10:307-313.

García-Plazaola JI, Fernández-Marín B, Ferrio JP, Alday JG, Hoch G, Landais D, Milcu A, Tissue DT, Voltas J, Gessler A, Roy J, Resco de Dios V (2017) Endogenous circadian rhythms in pigment composition induce changes in photochemical efficiency in plant canopies. Plant Cell Environ doi:10.1111/pce.12909.

Havaux M, Dall'Osto L, Bassi R (2007) Zeaxanthin has enhanced antioxidant capacity with respect to all other xanthophylls in Arabidopsis leaves and functions independent of binding to PSII antennae. Plant Physiol 145:1506-1520.

Havaux M, García-Plazaola JI (2014) Beyond non-photochemical fluorescence quenching: the overlapping antioxidant functions of zeaxanthin and tocopherols. In: Demmig-Adams B, Garab G, Adams W, Govindjee (eds) Non-photochemical quenching and energy dissipation in plants, algae and cyanobacteria. Springer, Dordrecht, The Netherlands. pp 583-603.

Kolari P, Lappalainen HK, Hänninen H, Hari P (2007) Relationship between temperature and the seasonal course of photosynthesis in Scots pine at northern timberline and in southern boreal zone. Tellus B 59: 542-552

Kouril R, Wientjes E, Bultema JB, Croce R, Boekema EJ (2013) High-light vs. low-light: effect of light acclimation on photosystem II composition and organization in Arabidopsis thaliana. Biochim Biophys Acta 1827:411-419.

Kromdijk J, Głowacka K, Leonelli L, Gabilly ST, Iwai M, Niyogi KK, Long SP (2016) Improving photosynthesis and crop productivity by accelerating recovery from photoprotection. Science 354:857-861.

Litthauer S, Battle MW, Lawson T, Jones MA (2015) Phototropins main- tain robust circadian oscillation of PSII operating efficiency under blue light. Plant J 83:1034-1045.

McClung (2006) Plant circadian rhythms. Plant Cell 18: 792-803

Míguez F, Fernández-Marín B, Becerril JM, García-Plazaola JI (2015) Activation of photoprotective winter photoinhibition in plants from different environments: a literature compilation and meta-analysis. Physiol Plant 155:414-423.

Míguez F, Fernández-Marín B, Becerril JM, García-Plazaola JI (2017) Diversity of winter photoinhibitory responses: a case study in co-occurring lichens, mosses, herbs and woody plants from subalpine environments. Physiol Plant doi:10.1111/ppl.12551

Morosinotto T, Bassi R (2012) Assembly of light harvesting pigment-protein complexes in photosynthetic eukaryotes. In: Eaton-Rye JJ, Tripathy BC, Sharkey TD (eds) Photosynthesis: Plastid Biology. Energy Conversion and Carbon Assimilation. Advances in Photosynthesis and Respiration 34. Springer, London. pp 113-126.

Pan WJ, Wang X, Deng YR, Li JH, Chen W, Chiang JY, Yang JB, Zheng L (2015) Nondestructive and intuitive determination of circadian chlorophyll rhythms in soybean leaves using multispectral imaging. Sci Reports 5:11108.

Patankar R, Mortazavi B, Oberbauer SF, Starr G (2013) Diurnal patterns of gas-exchange and metabolic pools in tundra plants during three phases of the arctic growing season. Ecol Evol 3:375-388.

Pedersen B (1990) Distributional patterns of vascular plants in Fennoscandia: a numerical approach. Nord. J. Bot 10: 163-189

Porcar-Castell A, Tyystjärvi E , Atherton J, van der Tol C , Flexas J, Pfündel EE, Moreno J, Frankenberg C, Berry JA (2014) Linking chlorophyll a fluorescence to photosynthesis for remote sensing applications: mechanisms and challenges. J Exp Bot 15:4065-4095.

Shmakova NY, Markovskayab EF (2010) Photosynthetic pigments of plants and lichens inhabiting arctic tundra of West Spitsbergen. Russ J Plant Physiol 57:764–769.

Velez-Ramirez AI, van Ieperen W, Vreugdenhil D, Millenaar FM (2011) Plants under continuous light. Trends Plant Sci 16:310-318.

Velez-Ramirez AI, van Ieperen W, Vreugdenhil D, Pieter MJA, van Poppel MJA, Heuvelink E, Millenaar FM (2014) A single locus confers tolerance to continuous light and allows substantial yield increase in tomato. Nat Commun 5:4549.

Zhao W, Wang S, Li X, Huang H, Sui X, Zhang Z (2012) Molecular cloning and characterization of the light-regulation and circadian-rhythm of the VDE gene promoter from *Zingiber officinale*. Plant Cell Rep 31:1381-1392.

Tables

Table 1. Summary of significant results after hierarchical (ordered) regression analysis for each of the three species studied. Three different models with increasing complexity were tested: M1, tested the influence of PPFD of the period of sampling plus the previous 30min; M2, PPFD plus temperature; M3, PPFD plus temperature plus time of the day (normalised solar zenith angle). "Delta r^2" indicates the increase in R^2 compared to the immediately simpler model (e.g. M2 vs M1, and M3 vs M2), and "model.p" indicates whether this increase was significant or not ($P<0.05$). Only significant models are shown (complete data set including non-significant models is available as supplementary material:

Species	Pigment	Model	r2.model	delta.r2	model.p	yi.est	yi.p	par.est	par.p	temp.est	temp.p	szen.inv.est	szen.inv.p
Alpine bearberry	Neo / Chl	M3	0,590	0,500	0,023	38,450	0,000	-0,003	0,070	-0,142	0,160	4,462	0,023
	α-Car / Chl	M3	0,630	0,480	0,020	0,620	0,016	-0,001	0,011	-0,003	0,880	0,863	0,020
Mountain birch	Ant / Chl	M1	0,680	0,680	0,006	7,700	0,000	0,011	0,002	NA	NA	NA	NA
	Zea /Chl	M1	0,520	0,520	0,013	0,320	0,001	0,000	0,012	NA	NA	NA	NA
Scots pine	Neo / Chl	M1	0,428	0,430	0,027	50,860	0,000	-0,006	0,029	NA	NA	NA	NA
	α-Car / Chl	M1	0,449	0,450	0,004	11,380	0,000	-0,002	0,024	NA	NA	NA	NA
	α–Car / Chl	M2	0,734	0,280	0,012	13,490	0,000	-0,001	0,069	-0,179	0,019	NA	NA
	β-Car / Chl	M1	0,522	0,520	0,008	155,400	0,000	-0,022	0,012	NA	NA	NA	NA
	Tot Car / Chl	M1	0,388	0,390	0,042	473,660	0,000	-0,058	0,041	NA	NA	NA	NA

Tables S3, S4, S5).

Figures

Fig. 1. Air temperature (°C) (in red) and PPFD (µmol m^{-2} s^{-1}) (in black) during the study period (June 21st at 13.00 h to 24th at 10.00 h) and the previous week. Inset shows detailed PPFD and temperature for the two complete daily cycles. The eleven sampling timepoints of study are highlighted with shaded rectangles. Note that the PPFD is shown with logarithmic scale in the inset, this allows better appreciation of lowest irradiance intensities.

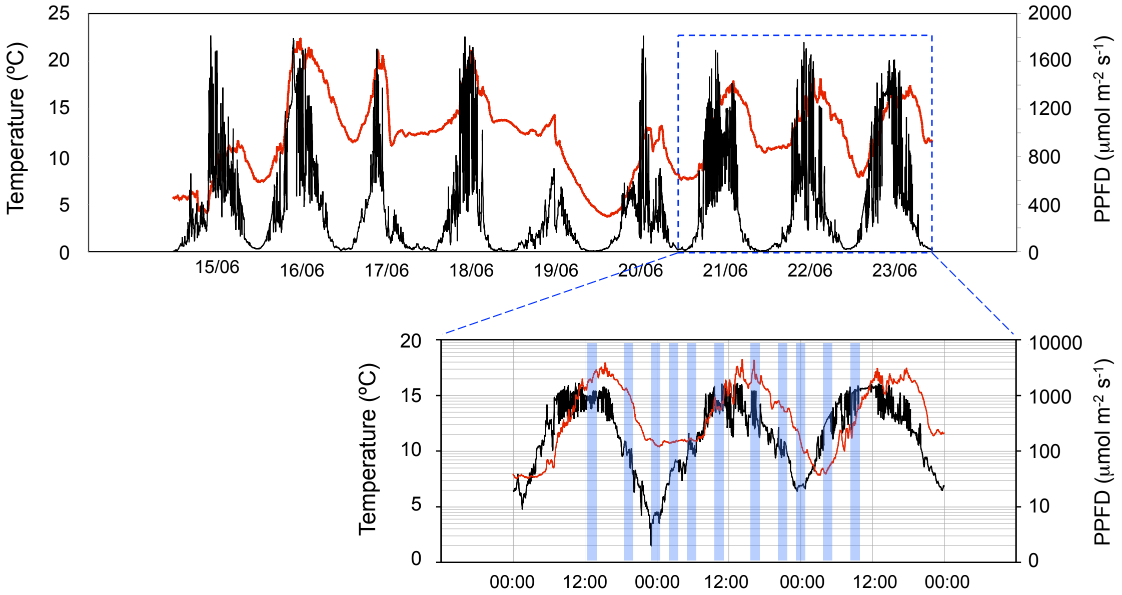

Fig. 2. Pigment composition in leaves of alpine bearberry, mountain birch and Scots pine. Data are averages of the 11 time points during the study. Letters above the bars indicate significant differences among species (P<0.05)

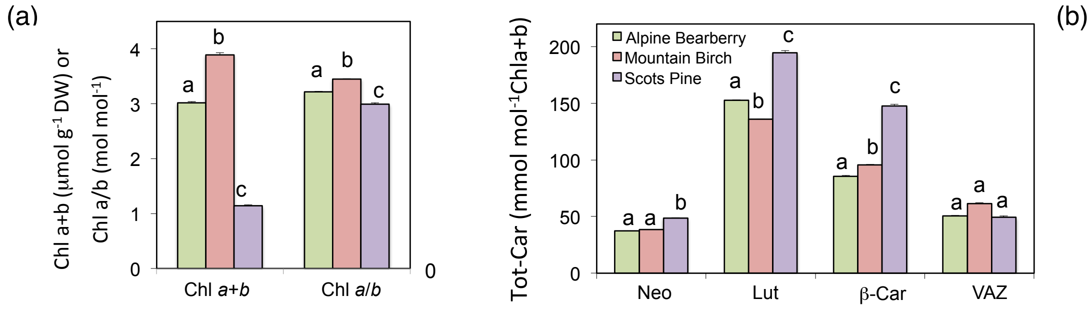

Fig. 3. Changes in total Chl, carotenoids to Chl and AZ/VAZ ratios along the study period (in hours). Triangles represent Scots pine, circles represent alpine bearberry and diamonds represent mountain birch. Black bars correspond with subjective night periods (6 hours around midnight). Data are the mean of 4 replicates ± SE.

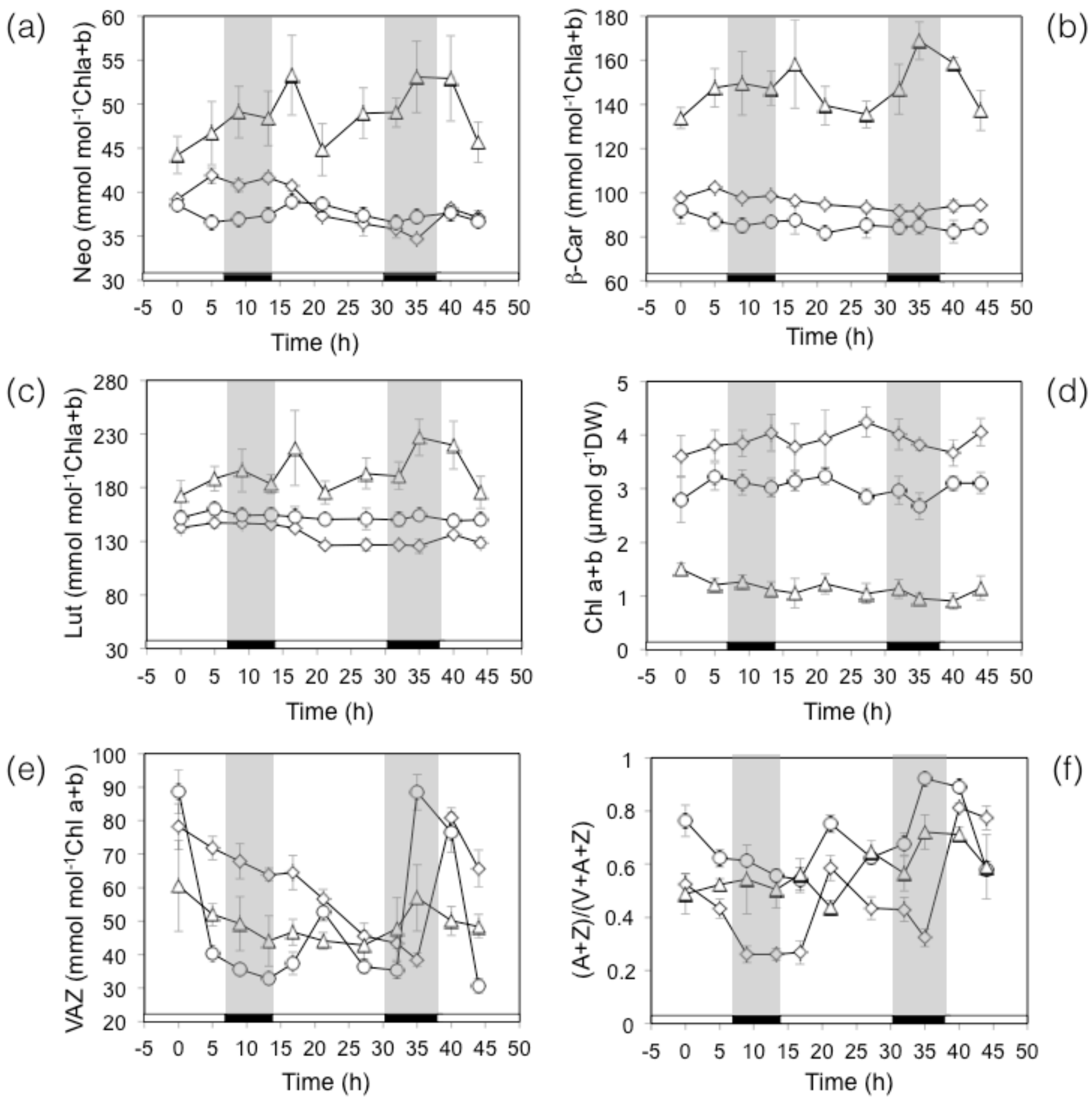

Fig. 4 Correlation matrices for environmental (including the circadian control variable: normalised solar angle), biochemical and photochemical variables for each of the species. Note: Mountain birch species lacks Lx and α-Car in its carotenoid composition.

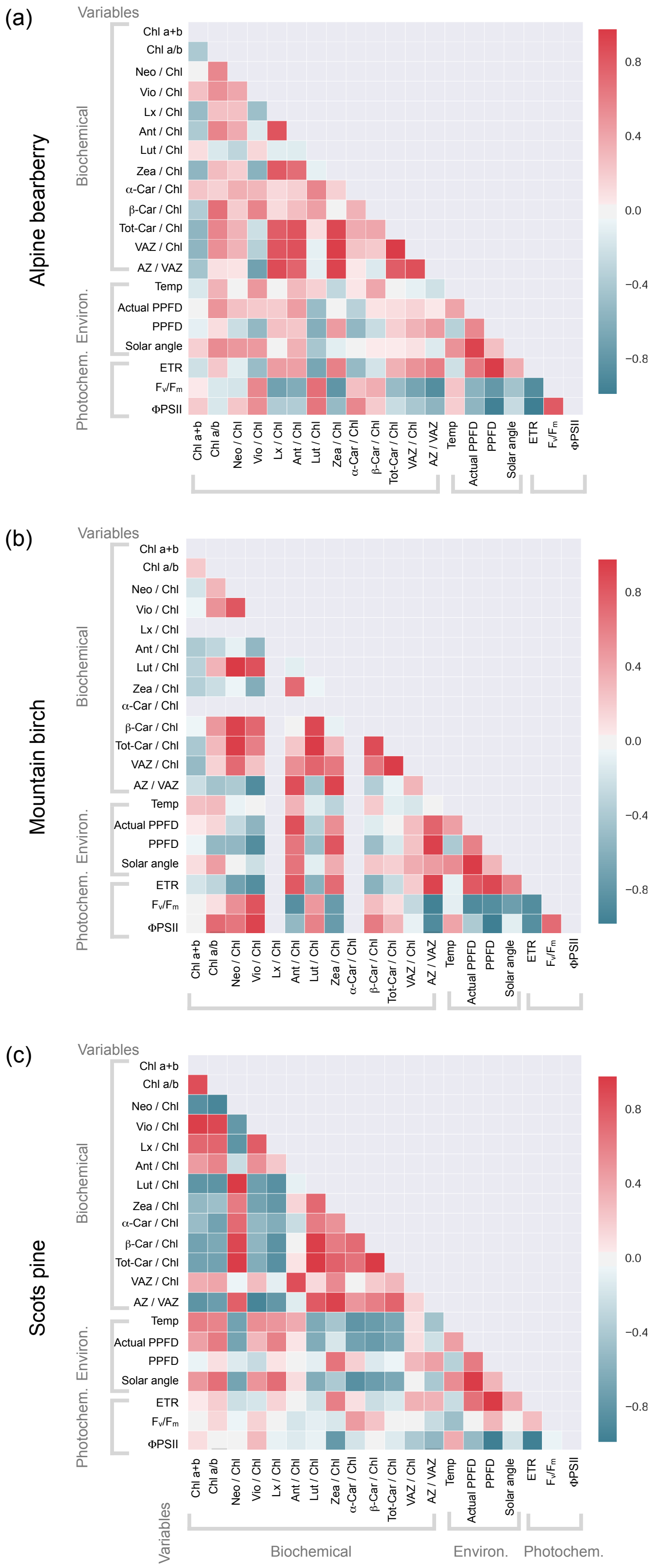

Fig. 5. Effect that a sunbeam, occurring at subjective night, had on the content of carotenoids. Panel (a): changes in PPFD during the transition from the 22nd to the 23rd of June. Panels (b-g): carotenoids content before (close bars) and after (open bars) the change in PPFD observed around 21:30 (EET). When significant, differences in the content of carotenoids before and after the sunbeam are depicted with letters above bars (*P*<0.05)

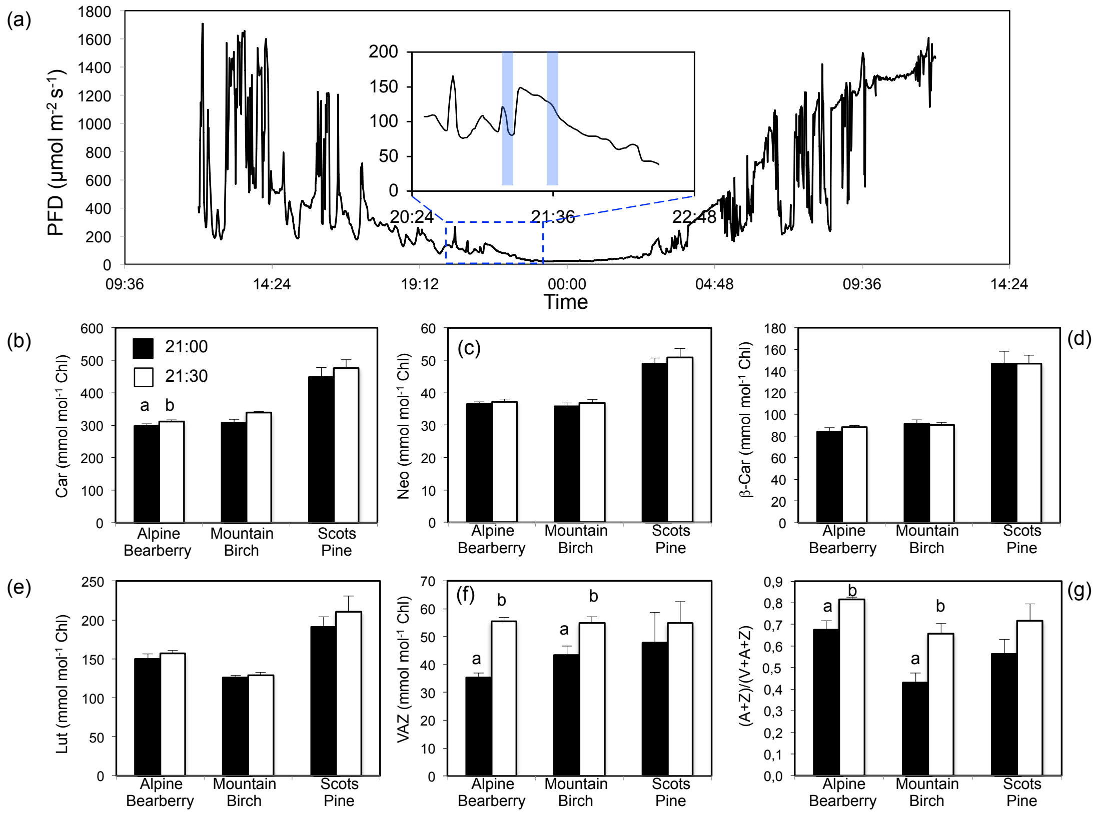

Fig. 6. Relationships between F_v/F_m and AZ/VAZ in the three species. Black circles represent measurements during the subjective night and empty circles represent daytime measurements. When correlations were significant, fit to a linear regression model, R^2 and P are shown inside the panel. Solid lines stand for daytime points and dashed lines for subjective night points.

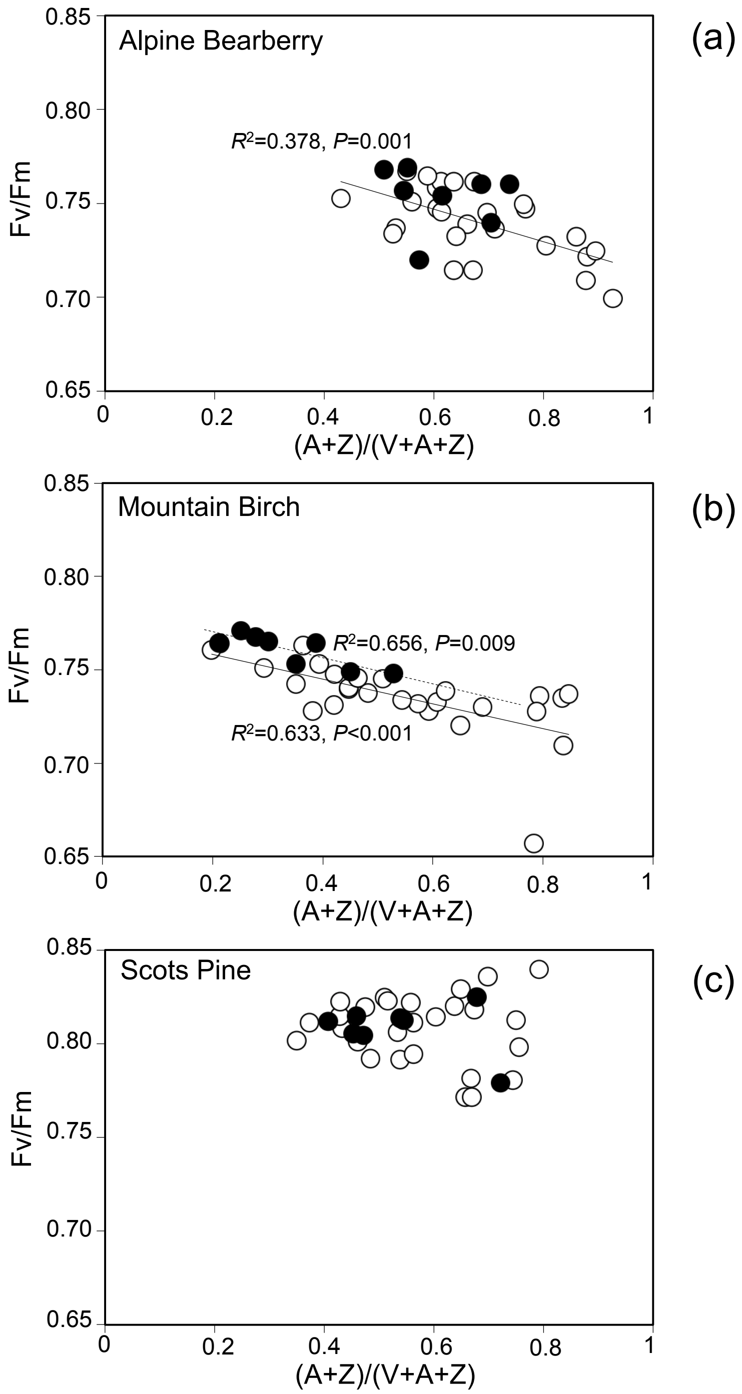

Fig. 7. Initial (linear) part of the response curve of ETR to “actual PPFD” (PPFD directly measured with the PAM2500 over each leaf under natural illumination, during ΦPSII measurement) in the three species. Black circles represent subjective night measurements and empty circles represent daytime measurements. Each symbol represents one measurement. Fit to a linear regression is shown as solid line for day points and as dashed red line for subjective night.

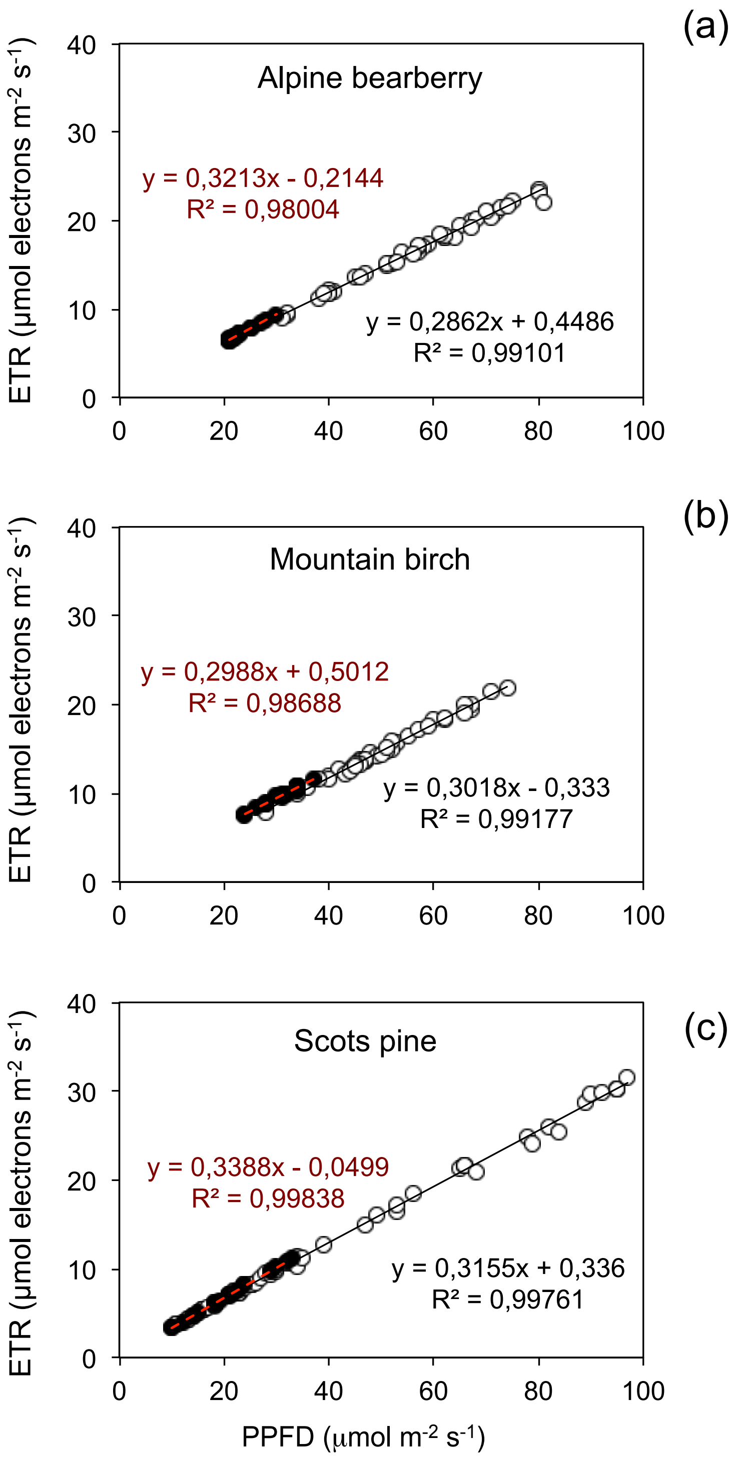

Fig. 8. Average response of CO_2 fluxes from Scots pine shoots during the summer solstice week from 2001 to 2016. Left: variation along the day during the daily cycle of CO_2 flux (a) and PPFD (b). Right: initial slope of the CO_2 flux vs. PPFD response during subjective night (c) and during daytime (d). Only values measured at temperatures in the range 10-15 °C were considered..

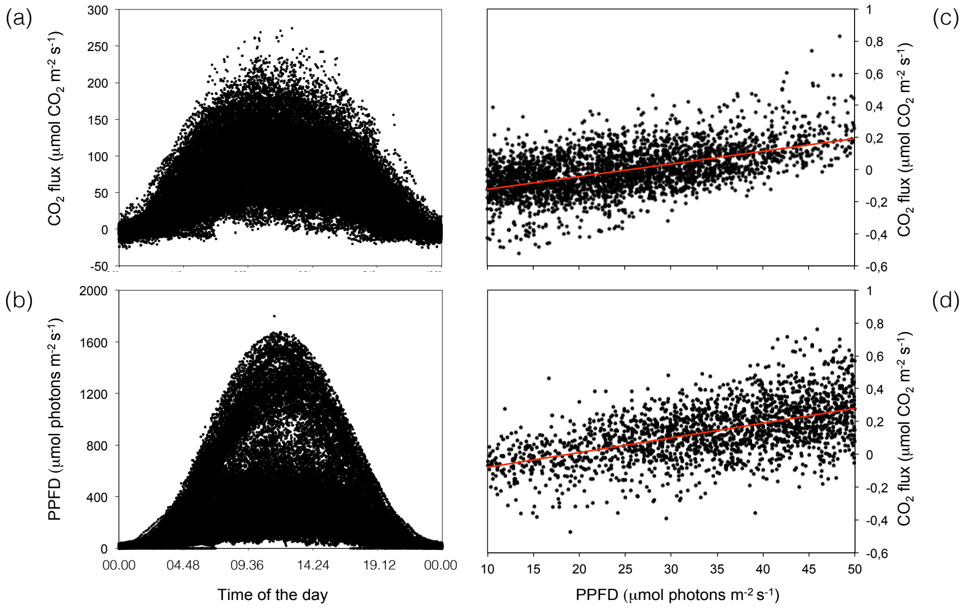

Supplementary Material

Table S1. Summary of the ANOVA for pigment contents along the experiment. Only for parameters for which the ANOVA was significant, the post hoc Duncan test result is shown.

	ANOVA Alpine bearberrry		DUNCAN					(Time of the experiment (h))						
Pigment	F	Sig	0	5	9	13,25	16,75	21,2	27,2	32	32,5	35	40	44
Neo /Chl	1,915	0,070												
b-Car / Chl	0,663	0,763												
Lut / Chl	0,369	0,960												
Chl a+b	1,250	0,292												
VAZ / Chl	**41,584**	**0,000**	a	b	b	b	b	c	b	b	c	ad	d	b
AZ/VAZ	**24,222**	**0,000**	a	bc	bc	b	b	a	bc	c	ad	e	de	b
	Mountain birch													
	F	Sig												
Neo /Chl	**12,178**	**0,000**	ab	c	bc	c	bc	ade	de	d	de	d	ae	ade
b-Car / Chl	**5,288**	**0,000**	abc	a	abc	ab	bcd	bcde	cde	de	e	e	bcde	bcde
Lut / Chl	**3,897**	**0,001**	ab	b	b	b	ab	c	c	c	ac	abc	abc	ac
Chl a+b	0,485	0,900												
VAZ / Chl	**15,325**	**0,000**	ab	abc	bc	cd	cd	d	fe	e	df	e	a	cd
AZ/VAZ	**24,632**	**0,000**	ab	bc	d	d	d	ae	bc	bc	e	c	f	f
	Scots pine													
	F	Sig												
Neo /Chl	1,239	0,299												
b-Car / Chl	1,454	0,193												
Lut / Chl	1,405	0,214												
Chl a+b	1,568	0,152												
VAZ / Chl	0,689	0,740												
AZ/VAZ	**2,396**	**0,025**	a	ab	ab	a	ab	a	ab	ab	b	b	b	ab

Table S2. Summary of the ANCOVA for the linear part of the PPFD vs ETR curve (i.e. PPFD<100 μmol photons m^{-2} s^{-1}).

		ANCOVA		
		F	Sig	Partial square
Alpine bearberry	Intersection	10,373	0,002	0,154
	PPFD	5985,973	0,000	0,991
	Day/Night	1,177	0,282	0,020
Mountain birch	Intersection	0,081	0,777	0,001
	PPFD	6661,038	0,000	0,992
	Day/Night	54,127	0,000	0,487
Scots pine	Intersection	25,962	0,000	0,252
	PPFD	31021,537	0,000	0,998
	Day/Night	1,005	0,319	0,013

Table S3. Summary of the ANCOVA result for the assessment of differences in the CO_2 assimilation of Scots pine at day vs. at subjective nighttime.

ANCOVA	F	Sig.	Partial square
Intersection	1069,129	0,000	0,175
PPFD	1963,852	0,000	0,281
Day/Night	**210,770**	**0,000**	**0,040**

Table S4. Hierarchical (ordered) linear regression analysis for Alpine bearberry. Three different models with increasing complexity were tested: M1, tested the influence of PPFD of the period of sampling and the previous 30min; M2, PPFD plus temperature; M3, PPFD plus temperature plus normalised solar zenith angle. "Delta r^2" indicates the increase in R^2 compared to the immediately simpler model (e.g. M2 vs M1, and M3 vs M2), and "model.p" indicates whether this increase was significant or not (P<0.05). Significant models are highlighted in bold.

Pigment	Model	r2.model	delta.r2	model.p	yi.est	yi.p	par.est	par.p	temp.est	temp.p	szen.inv.est	szen.inv.p
Chl a+b	M1	0.000	0.000	0.998	3.020	0.000	0.000	0.999	NA	NA	NA	NA
	M2	0.028	0.028	0.589	3.170	0.000	0.000	0.843	-0.012	0.640	NA	NA
	M3	0.380	0.350	0.085	3.270	0.000	-0.001	0.127	-0.029	0.250	0.800	0.085
Chl a/b	M1	0.260	0.260	0.156	3.170	0.000	0.000	0.112	NA	NA	NA	NA
	M2	0.280	0.020	0.673	3.120	0.000	0.000	0.220	0.005	0.650	NA	NA
	M3	0.290	0.014	0.723	3.130	0.000	0.000	0.862	0.003	0.790	0.074	0.723
Neo / Chl	M1	0.070	0.070	0.312	37.270	0.000	0.001	0.432	NA	NA	NA	NA
	M2	0.090	0.020	0.579	37.850	0.000	0.001	0.400	-0.049	0.690	NA	NA
	M3	**0.590**	**0.500**	**0.023**	**38.450**	**0.000**	**-0.003**	**0.070**	**-0.142**	**0.160**	**4.462**	**0.023**
Vio / Chl	M1	0.048	0.048	0.461	12.440	0.000	0.002	0.515	NA	NA	NA	NA
	M2	0.240	0.190	0.166	5.270	0.350	0.000	0.961	0.610	0.190	NA	NA
	M3	0.440	0.200	0.154	6.840	0.210	-0.010	0.195	0.370	0.410	11.508	0.154
Lx / Chl	M1	0.041	0.041	0.597	0.500	0.000	0.000	0.548	NA	NA	NA	NA
	M2	0.046	0.005	0.859	0.560	0.091	0.000	0.554	-0.005	0.850	NA	NA
	M3	0.051	0.005	0.854	0.540	0.130	0.000	0.693	-0.003	0.920	-0.088	0.854
Ant / Chl	M1	0.200	0.200	0.218	7.300	0.003	0.005	0.164	NA	NA	NA	NA
	M2	0.220	0.016	0.718	4.700	0.500	0.005	0.287	0.222	0.700	NA	NA
	M3	0.220	0.001	0.917	4.860	0.530	0.004	0.743	0.197	0.760	1.156	0.917
Lut / Chl	M1	0.250	0.250	0.111	154.000	0.000	-0.004	0.118	NA	NA	NA	NA
	M2	0.440	0.190	0.156	147.530	0.000	-0.006	0.043	0.551	0.140	NA	NA
	M3	0.480	0.040	0.487	148.160	0.000	-0.010	0.148	0.454	0.260	4.647	0.487
Zea / Chl	M1	0.000	0.000	0.984	27.300	0.016	0.000	0.983	NA	NA	NA	NA
	M2	0.100	0.100	0.404	57.670	0.120	0.009	0.688	-2.586	0.370	NA	NA
	M3	0.120	0.018	0.716	54.930	0.170	0.027	0.628	-2.166	0.510	-20.115	0.716
α-Car / Chl	M1	0.100	0.100	0.202	0.680	0.000	0.000	0.332	NA	NA	NA	NA
	M2	0.150	0.050	0.362	0.500	0.100	0.000	0.267	0.015	0.510	NA	NA
	M3	**0.630**	**0.480**	**0.020**	**0.620**	**0.016**	**-0.001**	**0.011**	**-0.003**	**0.880**	**0.863**	**0.020**
β-Car / Chl	M1	0.006	0.006	0.824	85.350	0.000	0.001	0.816	NA	NA	NA	NA
	M2	0.170	0.170	0.272	79.830	0.000	-0.001	0.763	0.470	0.240	NA	NA
	M3	0.180	0.002	0.905	79.960	0.000	-0.002	0.823	0.451	0.320	0.892	0.905
TotCar / Chl	M1	0.012	0.012	0.776	324.500	0.000	0.007	0.746	NA	NA	NA	NA
	M2	0.016	0.004	0.879	331.300	0.000	0.009	0.730	-0.579	0.870	NA	NA
	M3	0.016	0.000	0.969	331.670	0.000	0.007	0.923	-0.635	0.880	2.705	0.969
VAZ / Chl	M1	0.028	0.028	0.665	46.700	0.001	0.011	0.626	NA	NA	NA	NA
	M2	0.056	0.028	0.661	65.030	0.130	0.015	0.537	-1.561	0.640	NA	NA
	M3	0.058	0.002	0.901	63.930	0.180	0.023	0.725	-1.393	0.710	-8.070	0.901
AZ / VAZ	M1	0.004	0.004	0.871	0.680	0.000	0.000	0.859	NA	NA	NA	NA
	M2	0.065	0.062	0.512	0.830	0.006	0.000	0.652	-0.013	0.490	NA	NA
	M3	0.093	0.028	0.658	0.810	0.011	0.000	0.565	-0.010	0.650	-0.161	0.658

Table S5. Hierarchical (ordered) linear regression analysis for mountain birch. Three different models with increasing complexity were tested: M1, tested the influence of PPFD of the period of sampling and the previous 30min; M2, PPFD plus temperature; M3, PPFD plus temperature plus normalised solar zenith angle. "Delta r^2" indicates the increase in R^2 compared to the immediately simpler model (e.g. M2 vs M1, and M3 vs M2), and "model.p" indicates whether this increase was significant or not (P<0.05). Significant models are highlighted in bold.

Pigment	Model	r2.model	delta.r2	model.p	yi.est	yi.p	par.est	par.p	temp.est	temp.p	szen.inv.est	szen.inv.p
Chl a+b	M1	0.002	0.002	0.896	3.880	0.000	0.000	0.893	NA	NA	NA	NA
	M2	0.069	0.067	0.473	3.650	0.000	0.000	0.849	0.020	0.471	NA	NA
	M3	0.190	0.120	0.347	3.590	0.000	0.000	0.429	0.030	0.321	-0.475	0.350
Chl a/b	M1	0.021	0.021	0.679	3.450	0.000	0.000	0.674	NA	NA	NA	NA
	M2	0.080	0.059	0.488	3.410	0.000	0.000	0.938	0.003	0.493	NA	NA
	M3	0.230	0.150	0.287	3.420	0.000	0.000	0.343	0.001	0.792	0.093	0.290
Neo / Chl	M1	0.066	0.066	0.446	39.160	0.000	-0.002	0.444	NA	NA	NA	NA
	M2	0.069	0.002	0.882	38.570	0.000	-0.002	0.477	0.050	0.889	NA	NA
	M3	0.290	0.220	0.189	39.740	0.000	-0.010	0.142	-0.130	0.718	8.605	0.190
Vio / Chl	M1	0.280	0.280	0.101	38.980	0.000	-0.019	0.094	NA	NA	NA	NA
	M2	0.350	0.074	0.366	21.910	0.270	-0.024	0.070	1.453	0.367	NA	NA
	M3	0.450	0.094	0.310	26.010	0.210	-0.051	0.104	0.825	0.624	30.080	0.310
Ant / Chl	**M1**	**0.680**	**0.680**	**0.006**	**7.700**	**0.000**	**0.011**	**0.002**	**NA**	**NA**	**NA**	**NA**
	M2	0.680	0.001	0.868	8.530	0.110	0.011	0.005	-0.071	0.859	NA	NA
	M3	0.690	0.004	0.767	8.840	0.130	0.009	0.269	-0.119	0.794	2.296	0.770
Lut / Chl	M1	0.100	0.100	0.371	138.740	0.000	-0.008	0.331	NA	NA	NA	NA
	M2	0.110	0.001	0.919	137.150	0.000	-0.009	0.383	0.135	0.917	NA	NA
	M3	0.200	0.090	0.407	139.960	0.000	-0.028	0.277	-0.296	0.835	20.631	0.410
Zea / Chl	M1	0.260	0.260	0.078	11.090	0.066	0.019	0.110	NA	NA	NA	NA
	M2	0.570	0.320	0.057	47.160	0.016	0.029	0.016	-3.071	0.041	NA	NA
	M3	0.580	0.001	0.913	47.540	0.025	0.026	0.324	-3.129	0.066	2.794	0.910
β-Car / Chl	M1	0.012	0.012	0.742	95.980	0.000	-0.001	0.744	NA	NA	NA	NA
	M2	0.085	0.073	0.434	91.770	0.000	-0.002	0.543	0.358	0.448	NA	NA
	M3	0.260	0.180	0.238	93.160	0.000	-0.011	0.191	0.146	0.761	10.166	0.240
TotCar / Chl	M1	0.000	0.000	0.981	331.640	0.000	-0.001	0.980	NA	NA	NA	NA
	M2	0.011	0.011	0.769	345.100	0.000	0.003	0.919	-1.146	0.770	NA	NA
	M3	0.150	0.140	0.312	355.260	0.000	-0.065	0.374	-2.702	0.522	74.571	0.310
VAZ / Chl	M1	0.072	0.072	0.432	57.770	0.000	0.010	0.424	NA	NA	NA	NA
	M2	0.160	0.087	0.390	77.600	0.009	0.016	0.289	-1.688	0.389	NA	NA
	M3	0.270	0.110	0.331	82.400	0.009	-0.016	0.644	-2.423	0.259	35.170	0.330
AZ / VAZ	**M1**	**0.520**	**0.520**	**0.013**	**0.320**	**0.001**	**0.000**	**0.012**	**NA**	**NA**	**NA**	**NA**
	M2	0.660	0.140	0.131	0.670	0.010	0.000	0.004	-0.030	0.107	NA	NA
	M3	0.660	0.005	0.757	0.660	0.019	0.001	0.112	-0.028	0.181	-0.102	0.760

Table S5. Hierarchical (ordered) linear regression analysis for Scots pine. Three different models with increasing complexity were tested: M1, tested the influence of PPFD of the period of sampling and the previous 30min; M2, PPFD plus temperature; M3, PPFD plus temperature plus normalised solar zenith angle. "Delta r^2" indicates the increase in R^2 compared to the immediately simpler model (e.g. M2 vs M1, and M3 vs M2), and "model.p" indicates whether this increase was significant or not ($P<0.05$). Significant models are highlighted in bold.

Pigment	Model	r2.model	delta.r2	model.p	yi.est	yi.p	par.est	par.p	temp.est	temp.p	szen.inv.est	szen.inv.p
Chl a+b	M1	0.168	0.170	0.209	1.070	0.000	0.000	0.211	NA	NA	NA	NA
	M2	0.381	0.210	0.163	0.720	0.013	0.000	0.543	0.031	0.135	NA	NA
	M3	0.386	0.005	0.824	0.730	0.020	0.000	0.974	0.029	0.212	0.083	0.820
Chl a/b	M1	0.364	0.360	0.058	2.830	0.000	0.000	0.050	NA	NA	NA	NA
	M2	0.477	0.110	0.246	2.390	0.000	0.000	0.152	0.038	0.224	NA	NA
	M3	0.504	0.027	0.557	2.430	0.000	0.000	0.952	0.031	0.368	0.335	0.560
Neo / Chl	**M1**	**0.428**	**0.430**	**0.027**	**50.860**	**0.000**	**-0.006**	**0.029**	**NA**	**NA**	**NA**	**NA**
	M2	0.612	0.180	0.111	57.580	0.000	-0.004	0.098	-0.572	0.087	NA	NA
	M3	0.613	0.000	0.946	57.640	0.000	-0.005	0.459	-0.581	0.127	0.404	0.950
Vio / Chl	M1	0.090	0.090	0.330	19.020	0.000	0.004	0.371	NA	NA	NA	NA
	M2	0.265	0.180	0.187	9.720	0.200	0.001	0.762	0.792	0.204	NA	NA
	M3	0.428	0.160	0.201	11.620	0.130	-0.011	0.288	0.501	0.415	13.931	0.200
Lx / Chl	M1	0.333	0.330	0.069	1.770	0.000	0.000	0.063	NA	NA	NA	NA
	M2	0.396	0.063	0.384	1.410	0.009	0.000	0.167	0.031	0.390	NA	NA
	M3	0.492	0.096	0.288	1.510	0.008	0.000	0.693	0.016	0.662	0.693	0.290
Ant / Chl	M1	0.004	0.004	0.856	9.870	0.000	0.000	0.847	NA	NA	NA	NA
	M2	0.141	0.140	0.326	7.500	0.009	0.000	0.777	0.202	0.292	NA	NA
	M3	0.141	0.000	0.993	7.510	0.016	0.000	0.907	0.201	0.358	0.031	0.990
Lut / Chl	M1	0.354	0.350	0.059	205.500	0.000	-0.031	0.054	NA	NA	NA	NA
	M2	0.509	0.160	0.180	241.010	0.000	-0.022	0.171	-3.024	0.151	NA	NA
	M3	0.512	0.003	0.839	242.080	0.000	-0.029	0.465	-3.187	0.185	7.804	0.840
Zea / Chl	M1	0.024	0.024	0.607	19.850	0.000	-0.003	0.652	NA	NA	NA	NA
	M2	0.166	0.140	0.227	30.290	0.011	0.000	0.953	-0.888	0.276	NA	NA
	M3	0.430	0.260	0.115	27.280	0.014	0.021	0.139	-0.427	0.571	-22.082	0.110
α-Car / Chl	**M1**	**0.449**	**0.450**	**0.004**	**11.380**	**0.000**	**-0.002**	**0.024**	**NA**	**NA**	**NA**	**NA**
	M2	**0.734**	**0.280**	**0.012**	**13.490**	**0.000**	**-0.001**	**0.069**	**-0.179**	**0.019**	**NA**	**NA**
	M3	0.824	0.090	0.100	13.240	0.000	0.001	0.485	-0.141	0.043	-1.847	0.100
β-Car / Chl	**M1**	**0.522**	**0.520**	**0.008**	**155.400**	**0.000**	**-0.022**	**0.012**	**NA**	**NA**	**NA**	**NA**
	M2	0.727	0.200	0.054	179.120	0.000	-0.016	0.036	-2.020	0.040	NA	NA
	M3	0.733	0.006	0.706	179.970	0.000	-0.021	0.224	-2.150	0.055	6.261	0.710
TotCar / Chl	**M1**	**0.388**	**0.390**	**0.042**	**473.660**	**0.000**	**-0.058**	**0.041**	**NA**	**NA**	**NA**	**NA**
	M2	0.557	0.170	0.146	540.130	0.000	-0.041	0.134	-5.659	0.119	NA	NA
	M3	0.558	0.000	0.937	540.840	0.000	-0.045	0.498	-5.768	0.163	5.195	0.940
VAZ / Chl	M1	0.012	0.012	0.777	48.750	0.000	0.002	0.751	NA	NA	NA	NA
	M2	0.014	0.002	0.901	47.510	0.001	0.001	0.829	0.105	0.896	NA	NA
	M3	0.054	0.040	0.604	46.410	0.003	0.009	0.578	0.275	0.763	-8.120	0.600
AZ / VAZ	M1	0.041	0.041	0.525	0.590	0.000	0.000	0.551	NA	NA	NA	NA
	M2	0.179	0.140	0.260	0.750	0.001	0.000	0.935	-0.014	0.280	NA	NA
	M3	0.360	0.180	0.203	0.710	0.001	0.000	0.253	-0.008	0.540	-0.284	0.200